

Chapter 7

Magnetic hysteresis

Suggested Reading

For background:

Butler (1992), pp 48-54

To learn more:

O'Reilly (1984), pp 69-87

7.1 Introduction

In Lecture 4 we discussed the energies that control the state of magnetization within ferromagnetic particles. Particles will tend to find a configuration of internal magnetization directions that minimizes the energies (although meta-stable states with local energy minima or LEMs are a possibility). The longevity of a particular magnetization state has to do with the depth of the energy well that the magnetization is in and the energy available for hopping over barriers. We discussed a few basic configurations of the remanent magnetic state: uniform magnetization (single domain; SD), flower (F), vortex (V), and multi-domain (MD) states. We also mentioned the case in which thermal energy dominates: superparamagnetic (SP) particles.

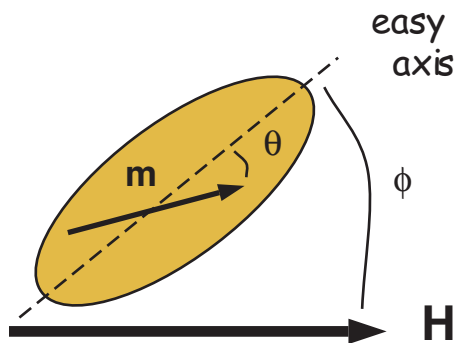


Figure 7.1: Sketch of a magnetic particle with easy axis as shown. In response to a magnetic field \mathbf{H} , applied at an angle ϕ to the easy axis, the particle moment \mathbf{m} rotates away from the easy axis, making an angle θ with the easy axis.

SP particles have sufficient thermal energy to easily overcome the various anisotropy energies;

they come into equilibrium with whatever external field they are in within minutes. Particles with domain walls (multi-domain, or MD particles) also have low stability. It is relatively easy to move a wall around within crystals so the domains grow and shrink depending on the external field unless they are pinned in some way.

Quasi-uniformly magnetized (SD and F states) particles have a great deal of resistance to changes in the external field because the magnetization vectors have to jump over high energy barriers to change directions within the crystal. These particles require relatively high magnetic fields to overcome the anisotropy energy and change their magnetizations. Finally, vortex state particles are somewhere in between the extremes of uniformly magnetized particles and those with domain walls.

The ease with which particles can be “coerced” into changing their magnetizations in response to external fields can tell us much about the overall stability of the particles and perhaps also something about their ability to carry a magnetic remanence over the long haul. The concepts of long term stability, incorporated into the concept of relaxation time and the response of the magnetic particles to external magnetic fields are therefore linked through the anisotropy energy constant K (see Lecture 4). In this lecture we will discuss the behavior of magnetic particles in response to external magnetic fields.

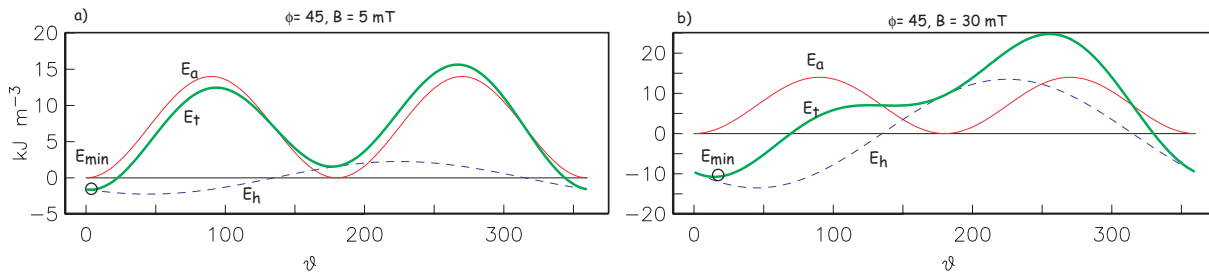


Figure 7.2: Variation of the anisotropy energy $E_a = K_u \sin^2\theta$, the interaction energy $E_h = -M_s B \cos(\phi - \theta)$ and the total energy $E_t = E_a + E_h$ as a function of θ for the particle shown in Figure 1. The θ associated with the minimum energy is indicated by E_{min} . a) $B = 5 \text{ mT}$. b) $B = 30 \text{ mT}$.

7.2 The “flipping” field

Magnetic remanence is the magnetization in the absence of an external magnetic field. If we imagine a particle with a single “easy” axis - a so-called “uniaxial” particle, the magnetization in the absence of a magnetic field will be aligned along one of the directions parallel to the easy axis and θ , the angle between the magnetic moment \mathbf{m} and the easy axis is zero (see Figure 7.1a). But if an external field is applied at an angle ϕ to the easy axis, there will be a competition between the anisotropy energy (tending to keep the magnetization parallel to the easy axis) and the interaction energy (tending to line the magnetization up with the external magnetic field). We showed in Lecture 4 that the total magnetic energy density of such a particle is given by:

$$E_t = K_u \sin^2\theta - M_s B \cos(\phi - \theta) \quad (7.1)$$

[Note that this equation is in the form of energy density, so moment is normalized by volume: M_s .]

7.2. THE “FLIPPING” FIELD

The magnetic moment of a uniaxial single domain grain will find the angle θ that is associated with the minimum total energy (E_{min} ; see Figure 7.2). For low external fields (e.g., 5 mT; Figure 7.2a), θ will be closer to the easy axis and for higher external fields (e.g., 30 mT; Figure 7.2b), θ will be closer to the applied field direction (ϕ).

When a magnetic field that is large enough to overcome the anisotropy energy is applied in a direction opposite to the magnetization vector, the moment will jump over the energy barrier and stay in the opposite direction when the field is switched off. The field necessary to accomplish this feat is called the *flipping field* (B_f) (also sometimes the “switching field”). Stoner and Wohlfarth (1948) showed that the flipping field can be found from the condition that $dE_t/d\theta = 0$ and $d^2E_t/d\theta^2 = 0$. We will call this the “flipping condition”. The necessary equations can be found by differentiating Equation 7.1:

$$\frac{dE}{d\theta} = 2K_u \sin \theta \cos \theta - M_s B \sin(\phi - \theta), \quad (7.2)$$

and again

$$\frac{d^2E}{d\theta^2} = 2K_u \cos(2\theta) + M_s B \cos(\phi - \theta). \quad (7.3)$$

Solving these two equations for B and using trigonometric trickery we get:

$$B_f = \frac{2K_u (1 - t^2 + t^4)^{\frac{1}{2}}}{M_s (1 + t^2)} = \frac{2K_u}{M_s} \frac{1}{(\cos \frac{2}{3}\phi + \sin \frac{2}{3}\phi)^{\frac{3}{2}}} \quad (7.4)$$

where $t = \tan^{\frac{1}{3}}\phi$. Here we have the derivation for the so-called “intrinsic coercivity” (B_k) when the dominant magnetic anisotropy constant is K_u and ϕ is zero, $B_k = 2\frac{K_u}{M_s}$ (introduced as “coercivity” in Lecture 4).

Using the parameters for magnetite ($K_u = 1.4 \times 10^4 \text{ Jm}^{-3}$ and $M_s = 4.8 \times 10^5 \text{ Am}^{-1}$) we get $B_f = 58 \text{ mT}$. We plot the behavior of Equations 7.1 - 7.3 in Figure 7.3. We see that the minimum in E_t occurs at an angle of $\theta = 180^\circ$ and that the first and second derivatives satisfy the flipping criterion by having a common zero crossing. There is no other field for which this is true (see, e.g., the case of a 30 mT field in Figure 7.3c,d).

We show the flipping field B_f versus ϕ in Figure 7.4. For ϕ parallel to the easy axis (zero), B_f is 62 mT as we found before. B_f drops steadily as the angle between the field and the easy axis increases, until an angle of 45° when B_f starts to increase again. B_f is undefined when $\phi = 90^\circ$, so when the field is applied at right angles to the easy axis, there is no field sufficient to flip the moment.

When a single domain, uniaxial particle is subjected to an increasing magnetic field the magnetization is gradually drawn into the direction of the applied field. If the flipping condition is not met, then the magnetization will return to the original direction when the magnetic field is removed. If the flipping condition is met, then the magnetization undergoes an irreversible change and will be in the opposite direction when the magnetic field is removed.

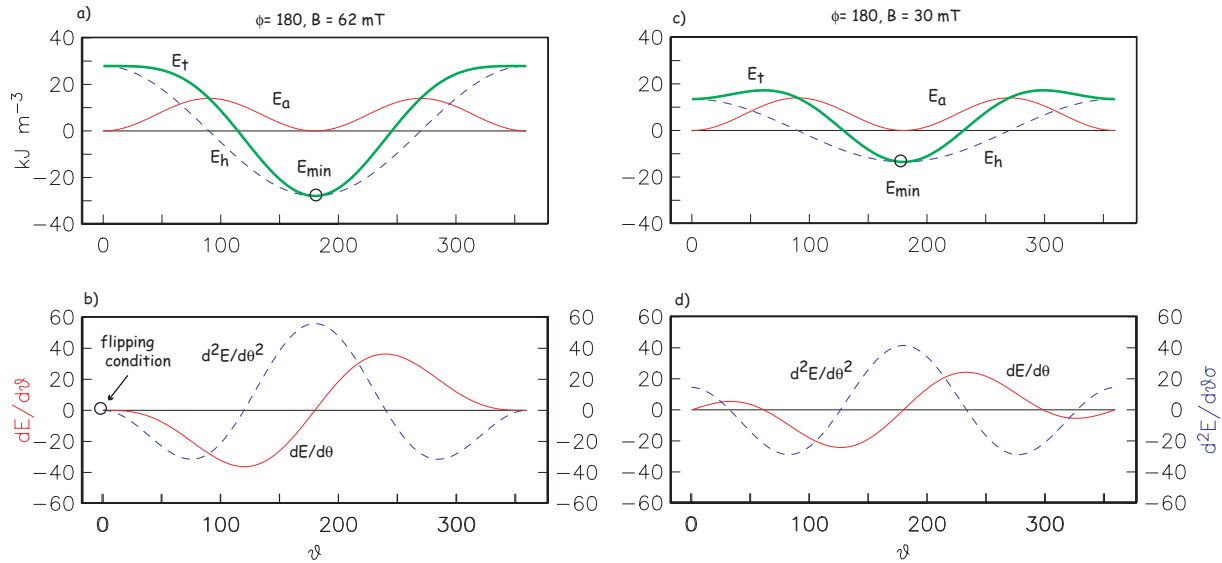


Figure 7.3: a) Variation of the anisotropy energy $E_a = K_u \sin^2\theta$, the interaction energy $E_h = -M_s B \cos \phi$ and the total energy $E_t = E_a + E_h$ as a function of θ for the particle shown in Figure 1. The field was applied with $\phi = 180^\circ$ and was 62 mT in magnitude. The θ associated with the minimum energy is indicated by E_{min} and is 180° . b) Variation in first and second derivatives of the energy equation. The flipping condition of both being zero simultaneously is met. c) Same a) but the field was only 30 mT. d) Same as b) but the flipping condition is not met.

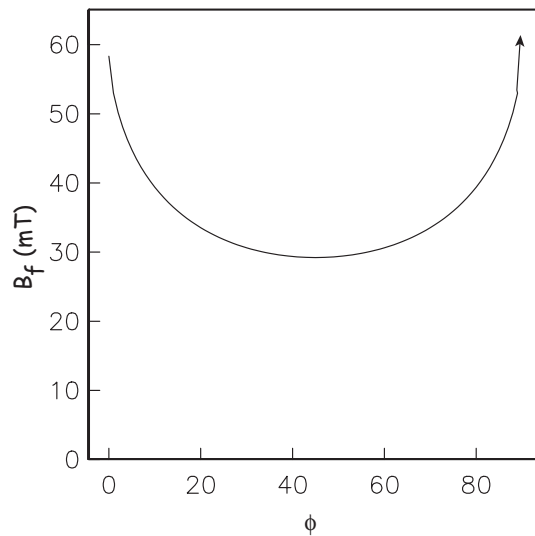


Figure 7.4: The flipping field B_f required to irreversibly switch the magnetization vector from one easy direction to the other in a single domain particle dominated by uniaxial anisotropy.

7.3. HYSTERESIS LOOPS

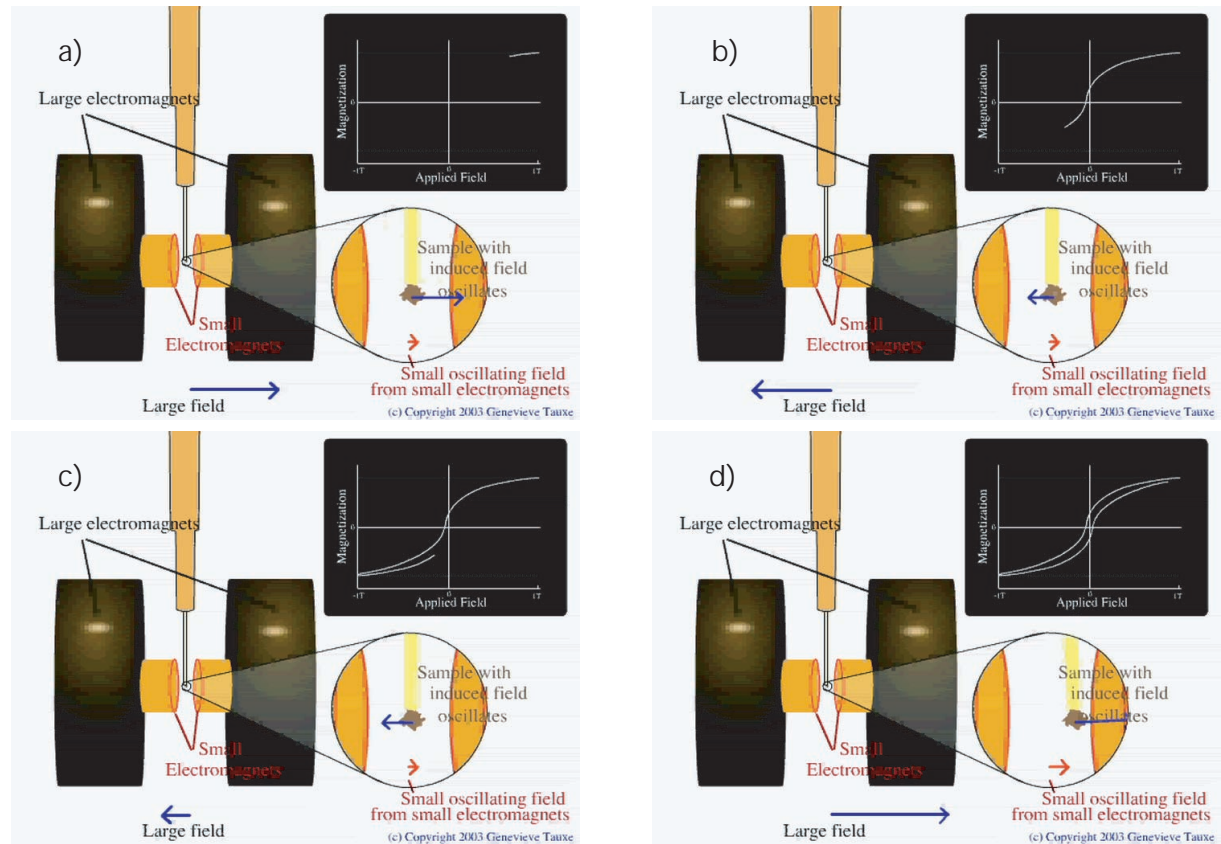


Figure 7.5: Making a hysteresis loop with an alternating gradient force magnetometer. A sample is hung between two small electromagnets that generate an oscillating field. These are set between the poles of a large electromagnet which generates a DC field in the direction of the blue arrow (labelled “large field”). The DC field induces a magnetic moment in the sample (shown as the inset) which vibrates with the oscillating field. The vibration is transmitted through the sample holder. The amplitude of the vibration is proportional to the induced magnetization. This is plotted against the applied large field in the hysteresis loop (upper right of figure). As the large field reduces, so does the induced field. b) After passing through zero, the DC field changes sign (shown by the blue arrow, bottom left of figure). At some field (the coercive field), the induced moment also changes sign (hysteresis loop upper right of figure). c) After reaching some maximum field, the DC field again changes sign and the magnetization begins its ascending loop (upper right diagram). d) As the DC field approaches its maximum, the hysteresis loop begins to close. [From animations by Genevieve Tauxe; see http://magician.ucsd.edu/Lab_tour/movs/agfm.mov.]

7.3 Hysteresis loops

Now let us consider what happens to single particles when subjected to applied fields in the cycle known as the “hysteresis loop”. Measurements of magnetic moment m as a function of applied field B are made on a variety of instruments, such as a vibrating sample magnetometer (VSM) or alternating gradient force magnetometer (AGFM; see Figure 7.5). In the AGFM, a sample is placed

on a thin stalk between pole pieces of a large magnet. There is a probe mounted behind the sample that measures the applied magnetic field. There are small coils on the pole pieces that modulate the gradient of the applied magnetic field (hence alternating gradient force). The sample vibrates in response to changing magnetic fields and the amplitude of the vibration is proportional to the moment in the axis of the applied field direction. The vibration of the sample stalk is measured and calibrated in terms of magnetic moment. The magnetometer is only sensitive to the induced component of \mathbf{m} parallel to the applied field \mathbf{H}_o , which is $m_{\parallel} = m \cos \phi$ (because the off axis terms are squared and very small, hence can be neglected.) In the hysteresis experiment, therefore, the moment parallel to the field m_{\parallel} is measured as a function of applied field B .

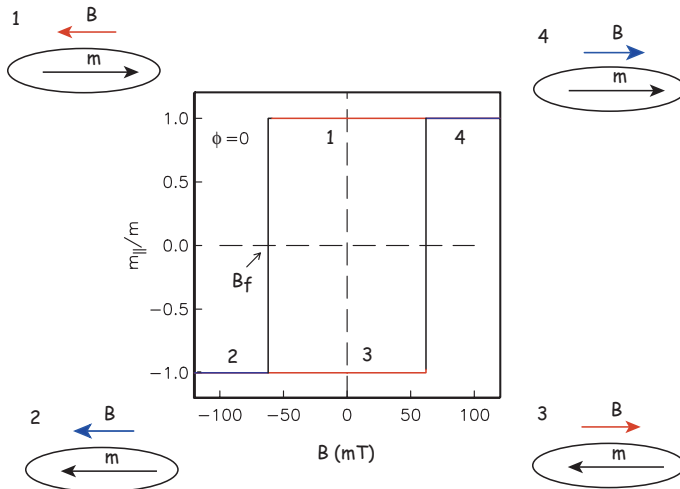


Figure 7.6: Moment measured for the particle ($\phi = 0^\circ$) with applied field starting at 0 mT and increasing in the opposite directions along track #1. When the flipping field B_f is reached, the moment switches to the other direction along track #2. The field then switches sign and decreases along track #3 to zero, then increases again to the flipping field. The moment flips and the the field increases along track #4.

A typical hysteresis experiment is shown in Figure 7.5. It takes a few minutes to complete such a loop. But understanding what the loops mean can take much more time and is the subject of the rest of the lecture.

7.3.1 Uniaxial anisotropy

Imagine a single domain particle with uniaxial anisotropy. Because the particle is single domain, the magnetization is at saturation and, in the absence of an applied field is constrained to lie along the easy axis. Now suppose we apply a magnetic field in the opposite direction (see track # 1 in Figure 7.6). When B reaches B_f in magnitude, the magnetization flips to the opposite direction (track #2 in Figure 7.6) and will not change regardless of how high the field goes. The field then is decreased to zero and then increased along track #3 in Figure 7.6 until B_f is reached again. The magnetization then flips back to the original direction (track #4 in Figure 7.6).

Applying fields at arbitrary angles to the easy axis results in loops of various shapes (see Figure 7.7a). As ϕ approaches 90° , the loops become thinner. Remember that the flipping fields for $\phi = 22^\circ$ and $\phi = 70^\circ$ are similar (see Figure 7.4) and are lower than that from $\phi = 0^\circ$, but the

7.3. HYSTERESIS LOOPS

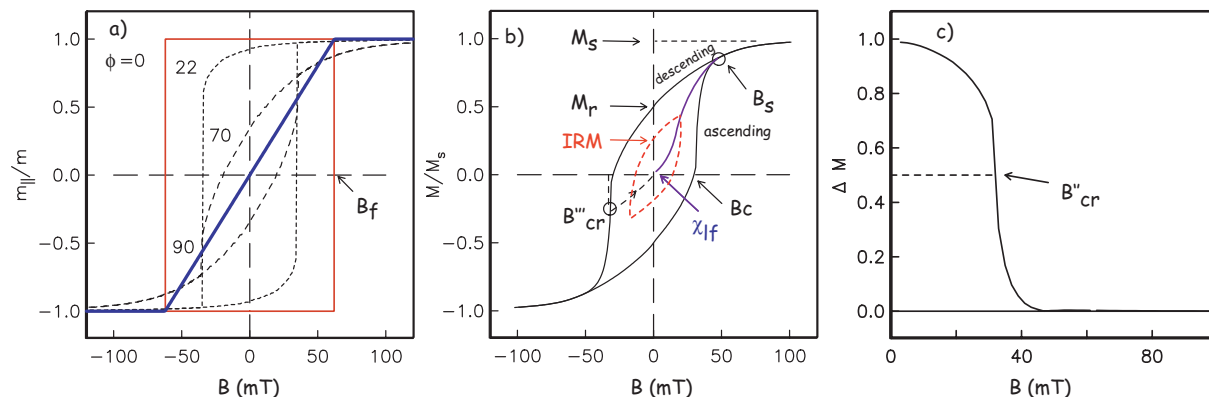


Figure 7.7: a) The component of magnetization parallel to $+B_{max}$ versus B for field applied with various angles ϕ . b) Sum of 10,000 individual curves similar to those shown in a) for ϕ drawn from a uniform distribution on a sphere. The saturation remanence M_r , bulk coercive field B_c and coercivity of remanence B'''_{cr} are indicated. If the measurements are made on a demagnetized specimen, increasing the field from zero, the initial slope is the low-field susceptibility. If the field returns to zero after some flipping fields have been exceeded, there is a net isothermal remanence (IRM). c) Ascending loop subtracted from the descending loop to make a ΔM curve. The field at which ΔM is 50% of the original is another measure of B_{cr} (labelled B''_{cr}). [Redrawn from Tauxe et al., 1996.]

flipping field for $\phi = 90^\circ$ is infinite, so that “loop” is closed and completely reversible.

In rocks with an assemblage of randomly oriented particles with uniaxial anisotropy, we would measure the sum of all the millions of tiny individual loops. A specimen from such a rock would yield a loop similar to that shown in Figure 7.7b. If the field is first applied to a demagnetized specimen, the initial slope is the (low field) magnetic susceptibility (χ_{lf}) first introduced in Lecture 1. From the treatment in Section 7.2 it is possible to derive the equation $\chi_{lf} = \mu_o M_s^2 / 3K_u$ for this initial (ferromagnetic) susceptibility (see O’Reilly 1984).

If the field is increased beyond the flipping field of some of the magnetic grains and returned to zero, the net remanence is called an isothermal remanence (IRM). If the field is increased to $+B_{max}$, all the magnetizations are drawn into the field direction and the net magnetization is equal to the sum of all the individual magnetizations and is the *saturation magnetization* M_s . When the field is reduced to zero, the moments relax back to their individual easy axes, many of which are at a high angle to the direction of the saturating field and cancel each other out. A loop that does not achieve a saturating field (red in Figure 7.7 is called a “minor hysteresis loop”, while one that does is called the “outer loop.”

The net remanence after saturation is termed the *saturation remanent magnetization* M_r (and sometimes the saturation isothermal remanence sIRM). For a random assemblage of single domain uniaxial particles, $M_r/M_s = 0.5$. The field necessary to reduce the net moment to zero is defined as the coercive field B_c .

The coercivity of remanence B_{cr} is defined as the magnetic field required to irreversibly flip half the magnetic moments (so the net remanence after application of $-B_{cr}$ to a saturation remanence is 0). B_{cr} is always greater than or equal to B_c and the ratio B_{cr}/B_c for our random assemblage of uniaxial SD particles is 1.09 (Wohlfarth, 1958). In Lecture 5 we introduced two ways of estimating

B_{cr} . Here we introduce two more ways. One is to use a so-called ΔM curve (Jackson et al. 1990). The ascending loop is subtracted from the descending loop. When all the moments are flipped into the new field, the ascending and descending loops join together and ΔM is 0. The field at which half the moments are flipped (the definition of coercivity of remanence), ΔM is at 50% of its initial value is here termed B''_{cr} (see Figure 7.7c). The other way of estimating B_{cr} is illustrated in Figure 7.7b. If one were to switch off the field at the point labeled B'''_{cr} , the magnetization would follow the dashed line and intersect the origin. For single domain grains, the dashed curve is parallel to the lower curve. So if one only measured the outer loop, one could estimate the coercivity of remanence by simply tracing the curve parallel to the lower curve (dashed line) from the origin to the point of intersection with the upper curve (circled in Figure 7.7b). This parameter is here called B'''_{cr} . This estimate is only valid for single domain grains.

7.3.2 Cubic anisotropy

In the case of equant grains of magnetite for which magnetocrystalline anisotropy dominates, there are four easy axes, instead of two as in the uniaxial case. The maximum angle ϕ between an easy axis and an applied field direction is 55° . Hence there is no individual loop that goes through the origin (see Figure 7.8). A random assemblage of particles with cubic anisotropy will therefore have a much higher saturation remanence. In fact, the theoretical ratio of M_r/M_s for such an assemblage is 0.87, as opposed to 0.5 for the uniaxial case (Joffe and Heuberger, 1974).

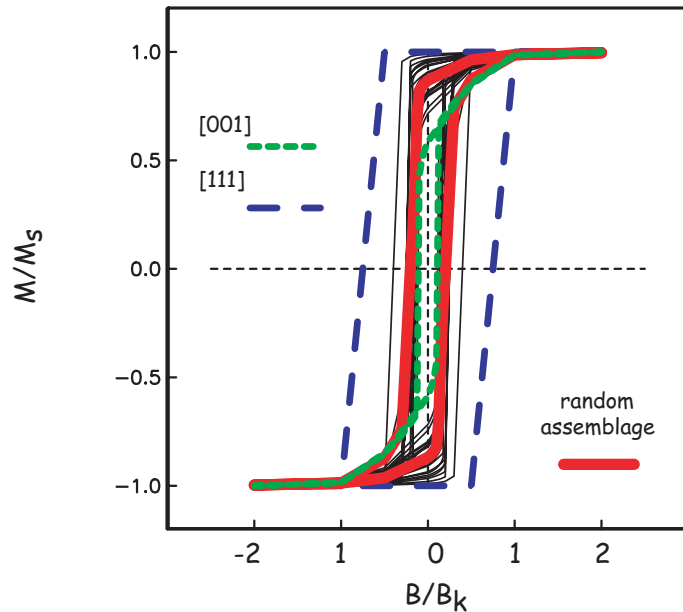


Figure 7.8: Heavy lines: theoretical behavior of cubic grains of magnetite. Dashed lines are the responses along particular directions. light grey lines: hysteresis response for single particles with various orientations with respect to the applied field. [Redrawn from Tauxe et al., 2002.]

7.3. HYSTERESIS LOOPS

7.3.3 SP particles

In superparamagnetic (SP) particles, E_t is balanced by thermal energy kT . This behavior can be modelled using statistical mechanics in a manner similar to that derived for paramagnetic grains in Lecture 3 and summarized in the Appendix. In fact,

$$\frac{M}{M_s} = N \left(\coth \gamma - \frac{1}{\gamma} \right). \quad (7.5)$$

where $\gamma = \frac{M_s B v}{kT}$ and N is the number of particles of volume v .

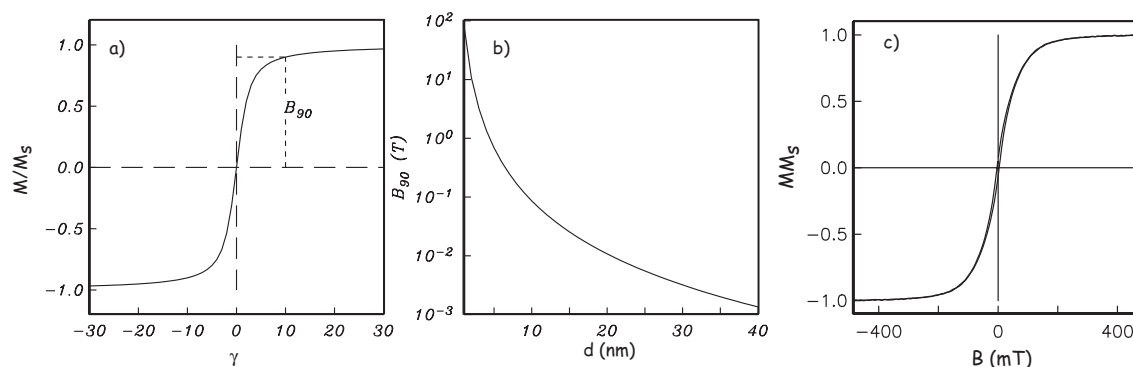


Figure 7.9: a) The contribution of SP particles with saturation magnetization M_s and cubic edge length d . $\gamma = BM_s d^3/kT$. There is no hysteresis. b) The field at which the magnetization reaches 90% of the maximum B_{90} is when $M_s d^3/kT \simeq 10$. (Figure redrawn from Tauxe et al., 1996.) c) Typical loop for a population of MD grains. (Data from gabbro from Troodos Ophiolite - courtesy of J.S. Gee).

Our end result, (Equation 7.5), is the familiar Langevin function from our discussion of paramagnetic behavior (Lecture 3); hence the term “superparamagnetic” for such particles.

The contribution of SP particles for which the Langevin function is valid with given M_s and d is shown in Figure 7.9a. The field at which the population reaches 90% saturation B_{90} occurs at $\gamma \sim 10$. Assuming particles of magnetite ($M_s = 4.8 \times 10^5$ A/m) and room temperature ($T = 300^\circ\text{K}$), B_{90} can be evaluated as a function of d (see Figure 7.9b). Because of its inverse cubic dependence on d , B_{90} rises sharply with decreasing d and is hundreds of tesla for particles a few nanometers in size, approaching paramagnetic values. The maximum size for SP behavior is rather controversial at the moment, but Tauxe et al. (1996) argue that it is ~ 20 nm.

For low magnetic fields, the Langevin function can be approximated as $\sim 1/3$. So we have:

$$\frac{M}{M_s} = \frac{1}{3} \frac{M_s B v}{kT}.$$

If we substitute $\mu_o H$ for B and rearrange this equation, we can get the superparamagnetic susceptibility χ_{sp} as:

$$\frac{M}{H} = \frac{\mu_o M_s v}{3kT}. \quad (7.6)$$

Remembering the equation for the blocking volume of a uniaxial crystal (Equation 5.8 in Lecture 5) as:

$$v_b = \frac{\ln(C\tau)}{K_u},$$

we can substitute this volume into Equation 7.6 as the maximum volume of an SP grain, giving us:

$$\chi_{sp} = \frac{\mu_o M_s^2 \ln(C\tau)}{3K_u}. \quad (7.7)$$

Comparing this expression with that derived for ferromagnetic susceptibility in Section 7.3.1, we find that χ_{sp} is a factor of $\ln(C\tau) \simeq 27$ larger than the equivalent single domain particle.

7.3.4 Vortex remanence state

Magnetite particles whose remanence states are in a “vortex” structure (see Lecture 4) probably flip using what has been called a “curling” mode. In order to flip its magnetic moment, the particle forms vortices which can zip through the particle. The hysteresis behavior of these particles can be modelled numerically (e.g. Tauxe et al., 2002). Examples of simulations of uniformly distributed assemblages are shown in Figure 7.10.

In Figure 7.10a we show the results from equant particles with widths of about 90 nm. The thin lines are individual loops for a given orientation of the applied field with respect to the crystallographic axes and the average loop is the heavy line. The loop from a uniform assemblage of such particles has a remanence ratio (M_r/M_s) of 0.63 and a coercive field of 14 mT. The expected values are 0.87 and 10 mT respectively for uniformly magnetized equant (CSD) particles of magnetite, so this flower state assemblage has a magnetization that is “harder”. The lower M_r/M_s ratio stems from the fact that the particles are not at saturation.

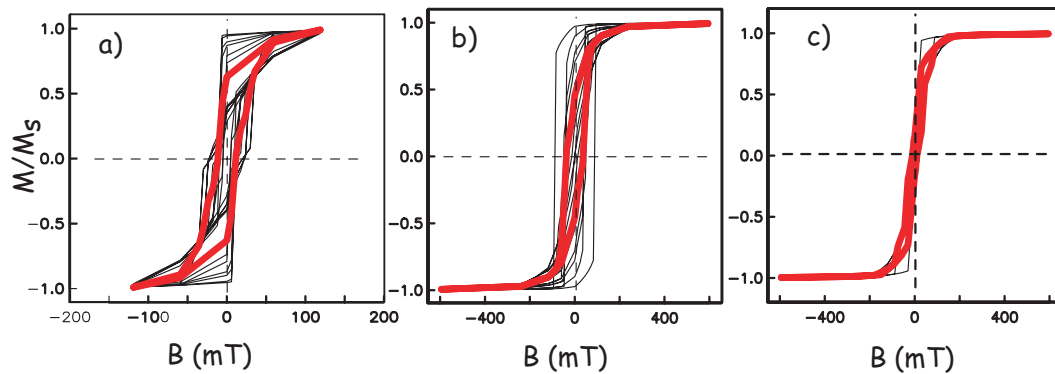


Figure 7.10: Simulated loops for assemblages of randomly oriented particles. a) Simulation of a 90 nm cubic particle. Thin lines are representative examples for various orientations of \mathbf{B} with respect to the crystallographic axes. Heavy line is the average loop for a random assemblage of particles. b) Same as a) but for a 70x140 nm parallelepiped. c) Same as a) but for a 115 nm cube. [Figure from Tauxe et al., 2002.]

In Figure 7.10b we show a similar set of curves for an assemblage of 70 nm particles with a/b ratios of 2. The remanence ratio of this assemblage is 0.46 and the coercive field is ~ 38 mT as compared to 0.5 and 69 mT. These uniaxial, flower state particles therefore have lower coercive fields than expected from a random assemblage of SD grains.

A third example of an assemblage of particles is shown in Figure 7.10c. This is for an assemblage of 115 nm (vortex state) equant particles. The average loop has a squareness of 0.16 and coercive field of 10 mT. Particles with characteristic vortex remanence states therefore have lower coercive

7.3. HYSTERESIS LOOPS

fields than SD particles, but higher than particles with domain walls discussed in the next section. They also have remanence ratios that are in between SD and MD particles.

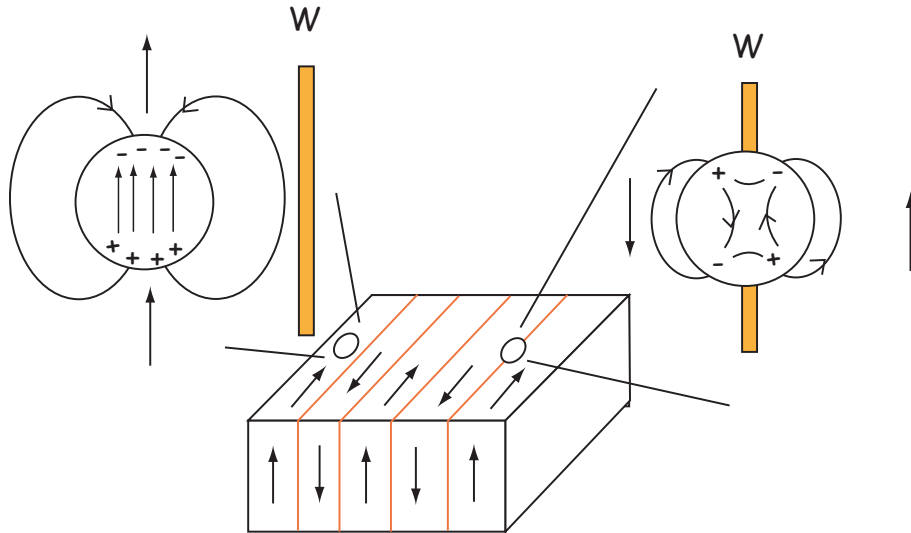


Figure 7.11: Interaction of a domain wall and a void. When the void is within a domain, free poles create a magnetic field which creates a self energy (Lecture 4). When a domain wall intersects the void, the self-energy is reduced. There are no exchange or magnetocrystalline anisotropy energy terms within the void, so the wall energy is reduced.

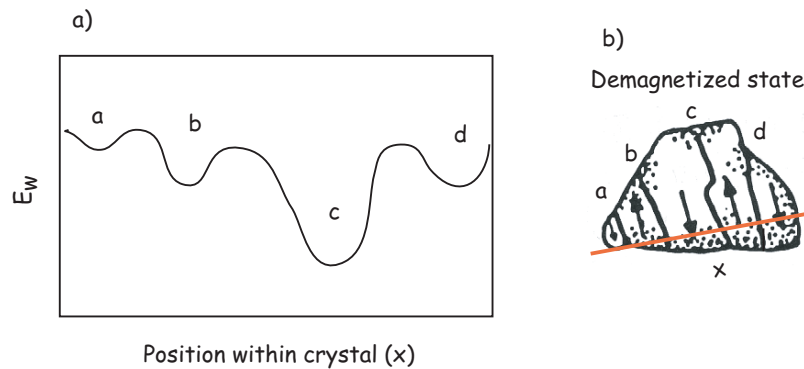


Figure 7.12: a) Schematic view of wall energy across a transect of a multi-domain grain. b) Placement of domain walls in the demagnetized state. [Domain observations from Halgedahl and Fuller, 1983.]

7.3.5 Particles with domain walls

Moving domain walls around is much easier than flipping the magnetization of an entire particle coherently. The reason for this is the same as the reason that it is easier to move a rug by lifting up a small wrinkle and pushing that through the rug, than to drag the whole rug by the same amount. Because of the greater ease of changing magnetic moments in MD grains, they have lower coercive fields and saturation remanence is also much lower than for uniformly magnetized particles (see Figure 7.9c). For grains large enough to have many walls (say a few microns), we predict that the grains would have no stability and the loop would be nearly indistinguishable from an SP loop. Yet some large grains have rather large coercivities and remanence ratios. The principle mechanism invoked to explain the unexpected stability of some grains is that wall energy is not uniform through-out the grain; some places have substantially lower energies than others and walls get “stuck” in these local energy minima (LEMs).

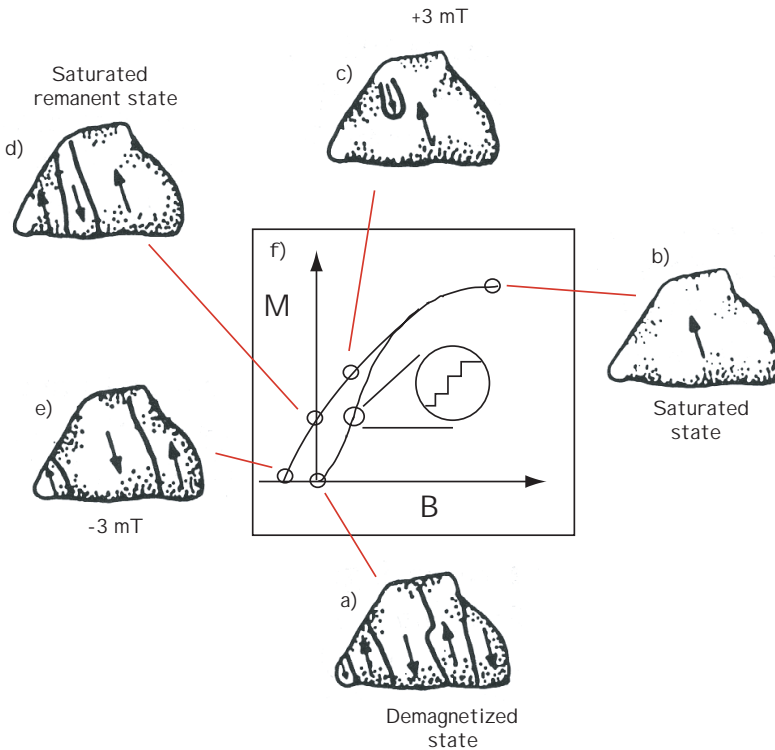


Figure 7.13: Schematic view of the magnetization process in MD grain shown in previous figure. a) Demagnetized state, b) in the presence of a saturating field, c) field lowered to +3 mT, d) remanent state, e) backfield of -3 mT, f) resulting loop. Inset shows detail of domain walls moving by small increments called Barkhausen jumps. (Domain wall observations from Halgedahl and Fuller, 1983; schematic loop after O’Reilly, 1984.)

There are several possible causes of variability in wall energy within a magnetic grain, for example, voids, lattice dislocations, stress, etc. The effect of voids is perhaps the easiest to visualize, so we will consider voids as an example of why wall energy varies as a function of position within the grain. We show a particle with lamellar domain structure and several voids in Figure 7.11. When the void occurs within a uniformly magnetized domain (left of figure), the void sets up a

7.3. HYSTERESIS LOOPS

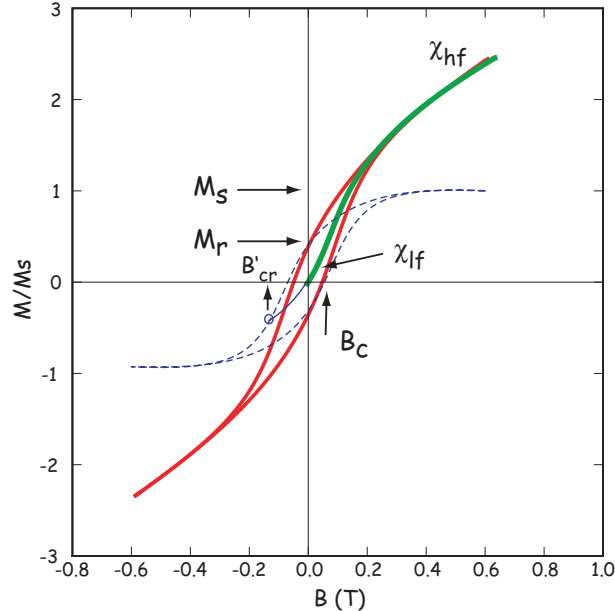


Figure 7.14: Heavy green line: initial behavior of demagnetized specimen as applied field ramps up from zero field to a saturating field. The initial slope is the initial or low-field susceptibility χ_{lf} . After saturation is achieved the slope is the high-field susceptibility χ_{hf} which is the non-ferromagnetic contribution, in this case the paramagnetic susceptibility (because χ_{hf} is positive). The dashed blue line is the hysteresis loop after the paramagnetic slope has been subtracted. Saturation magnetization M_s is the maximum value of magnetization after slope correction. Saturation remanence M_r is the value of the magnetization remaining in zero applied field. Coercivity (B_c) and coercivity of remanence B_{cr} are as in Figure 7.7

demagnetizing field as a result of the free poles on the surface of the void. There is therefore, a self-energy associated with the void. When the void is traversed by a wall, the free pole area is reduced, reducing the demagnetizing field and the associated self-energy. Therefore, the energy of the void is reduced by having a wall bisect it. Furthermore, the energy of the wall is also reduced, because the area of the wall in which magnetization vectors are tormented by exchange and magnetocrystalline energies is reduced. The wall gets a “free” spot if it bisects a void. The wall energy E_w therefore is lower as a result of the void.

In Figure 7.12, we show a sketch of a hypothetical transect of E_w across a particle. There are four LEMs labelled a-d. Domain walls will distribute themselves through out the grain in order to minimize the net magnetization of the grain and also to try to take advantage of LEMs in wall energy.

Domain walls move in response to external magnetic fields (see Figure 7.13). Starting in the demagnetized state (Figure 7.13a), we apply a magnetic field that increases to saturation (Figure 7.13b). As the field increases, the domain walls move in sudden jerks as each successive local wall energy high is overcome. This process, known as *Barkhausen jumps*, leads to the stair-step like increases in magnetization (shown in the inset of Figure 7.13). At saturation, all the walls have been flushed out of the crystal and it is uniformly magnetized. When the field decreases again, to say +3 mT (Figure 7.13c), domain walls begin to nucleate, but because the energy of

nucleation is larger than the energy of denucleation, the grain is not as effective in cancelling out the net magnetization, hence there is a net saturation remanence (Figure 7.13d). The walls migrate around as a magnetic field is applied in the opposite direction (Figure 7.13e) until there is no net magnetization). The difference in nucleation and denucleation energies was called on by Halgedahl and Fuller (1983) to explain the high stability observed in some large magnetic grains.

7.4 Magnetic susceptibility

Figure 7.7b showed the idealized case in which only ferromagnetic particles participated in the hysteresis measurements; in fact the curve is entirely theoretical. In “real” specimens there can be paramagnetic, diamagnetic AND ferromagnetic particles and the loop may well look like that shown in Figure 7.14. The initial slope of a hysteresis experiment starting from a demagnetized state in which the field is ramped from zero up to higher values is the low field magnetic susceptibility or χ_{lf} (see Figure 7.14a). If the field is then turned off, the magnetization will return again to zero. But as the field increases passed the lowest flipping field, the remanence will no longer be zero but some isothermal remanence (see Lecture 5). Once all particle moments have flipped and saturation magnetization has been achieved, the slope relating magnetization and applied field reflects only the non-ferromagnetic (paramagnetic and/or diamagnetic) susceptibility, here called χ_{hf} . In order to estimate the saturation magnetization and the saturation remanence, we must first subtract the high field slope. So doing gives us the blue dashed line from which we may read the various hysteresis parameters first defined in Figure 7.7b.

7.5 First Order Reversal Curves

Hysteresis loops can yield a tremendous amount of information yet much of this is lost by simply estimating the set of parameters $M_r, M_s, B_{cr}, B_c, \chi_i, \chi_{hf}$, etc.. Pike et al. (e.g., 1999) popularized the method of Mayergoyz (1986) or using so-called *First Order Reversal Curves* or FORCs to represent hysteresis data. In the FORC experiment, a sample is subjected to a saturating field, as in most hysteresis experiments. The field is lowered to some field H_a , then increased again through some value H_b to saturation (see Figure 7.15a). [It is unfortunate that the FORC terminology has chosen to use H_a , yet routinely neglects the necessary μ_o to render these field values in tesla...] The magnetization curve between H_a and H_b is a “FORC”. A series of FORCs (see Figure 7.15b) are generated to the desired resolution.

To transform FORC data into some useful form, they are gridded as in the inset in Figure 7.15c. In this example, we take a curve (in red) with its three neighbors on either side (in green), for a smoothing factor of $SF = 3$. The data in the box are fit with a polynomial surface of the form:

$$a_1 + a_2H_a + a_3H_a^2 + a_4H_b + a_5H_b^2 + a_6H_aH_b$$

where the a_i are fitted coefficients. The coefficient $-a_6(H_a, H_b)$ is contoured as in the Figure 7.15b and is a good approximation for the second derivative of the polynomial surface at P (Figure 7.15b). A FORC diagram is the contour plot rotated such that $H_c = (H_b - H_a)/2$ and $H_u = (H_a + H_b)/2$. Please note that because $H_a < H_b$, data are only possible for positive H_c .

7.5. FIRST ORDER REVERSAL CURVES

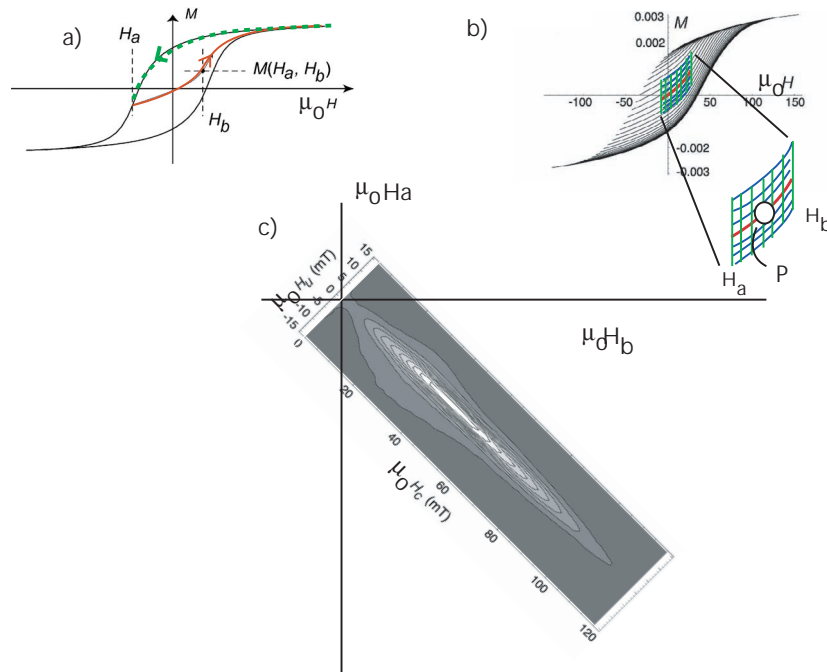


Figure 7.15: a) Dashed line is the descending magnetization curve taken from a saturating field to some field H_a . Red line is the first order reversal curve (FORC) from H_a returning to saturation. At any field $H_b > H_a$ there is a value for the magnetization $M(H_a, H_b)$. b) A series of FORCs for a single domain assemblage of particles. At any point “P” there are a set of related curves making a 7×7 grid. A polynomial surface is fit to these data is estimated. c) A contour plot of the mixed second derivative of the polynomial surface evaluated for points H_a, H_b . (Redrawn from Pike et al., Phys. Earth Planet. Int., 126, 11-25. 2001). Note: all H s are actually $\mu_0 H$.

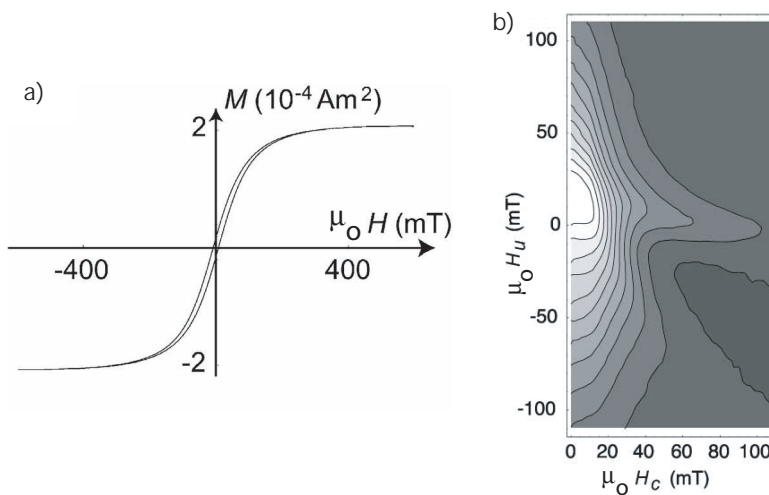


Figure 7.16: a) Hysteresis loop for a large, stressed grain of magnetite prior to annealing. b) FORC diagram from same. (Redrawn from Pike et al., 2001).

Imagine we travel down the descending magnetization curve (dashed line in Figure 7.15a) to a particular field $\mu_o H_a$ less than the smallest flipping field in the assemblage. If the particles are single domain, the behavior is reversible and the first FORC will travel back up the descending curve. It is only when $|\mu_o H_a|$ exceeds the flipping field of some of the particles that the FORC will trace a new curve on the inside of the hysteresis loop. In the simple single domain, non-interacting, uniaxial magnetite case, the FORC density in the quadrants where H_a and H_b are of the same sign must be zero. Indeed, FORC densities will only be non-zero for the range of flipping fields because these are the bounds of the flipping field distribution. So the diagram in Figure 7.15c is nearly that of an ideal uniaxial SD distribution.

Consider now the case in which a particle has domain walls. Walls can move much more easily than flipping the moment of an entire grain coherently. In fact, they begin to move in small jumps (from LEM to LEM) as soon as the applied field changes. If a wall nucleates while the field is decreasing and the field is then ramped back up, the magnetization curve will not be reversible, even though the field never changed sign or approached the flipping field for coherent rotation. The resulting FORC for such behavior would have much of the action in the region where H_a is positive. When transformed to H_u and H_c , the diagram will have the highest densities for small H_c but over a range of $\pm H_u$ as shown in Figure 7.16.

7.5.1 Which FORC should you use?

FORC diagrams take hours to create while a single hysteresis loop takes minutes. In many cases the the most interesting thing one learns from FORC diagrams is the degree to which there is irreversible behavior when the field is reduced to zero then ramped back up to saturation (see Figure 7.17). Such irreversible behavior in what Yu and Tauxe (2004) call the “Zero FORC” or ZFORC can arise from particle interactions, domain wall jumps or from the formation and destruction of vortex structures in the magnetic grains.

Fabian (2003) defined a parameter called “transient hysteresis” which is the area between the ascending and descending loops of a ZFORC (shaded area in Figure 7.17). This is defined as:

$$TH = \sum_0^{B_s} [M_{descending} - M_{ascending}] \cdot \Delta B.$$

where ΔH is the field increment used in the hysteresis measurement. When normalized by M_s , TH has units of B (tesla).

Transient hysteresis is thought to result from self demagnetization, for example shifting of domain walls or the formation and destruction of vortex structures. An example of what might be causing transient hysteresis at the macro scale is shown for micromagnetic modelling of a single particle in Figure 7.17b (Yu and Tauxe, 2004). The ZFORC starts and ends at saturation. On the descending loop, a vortex structure suddenly forms, at the point on the hysteresis loop labelled a), sharply reducing the magnetization. The magnetization state just before the jump is shown as snapshot labelled “descending branch”. The vortex remains along the ascending branch until much higher fields (see snapshot labelled “ascending branch”). The irreversible behavior of millions of particles with different sizes and shapes leads to the total transient hysteresis of the macro specimen. In general, Tauxe and Yu (2004) showed that the larger the particle, the greater the transient hysteresis, until truly multi-domain behavior essentially closed the loop, precluding the observation of TH (or of a FORC diagram for that matter).

7.6. A GLIMPSE AT PARTICLE INTERACTION

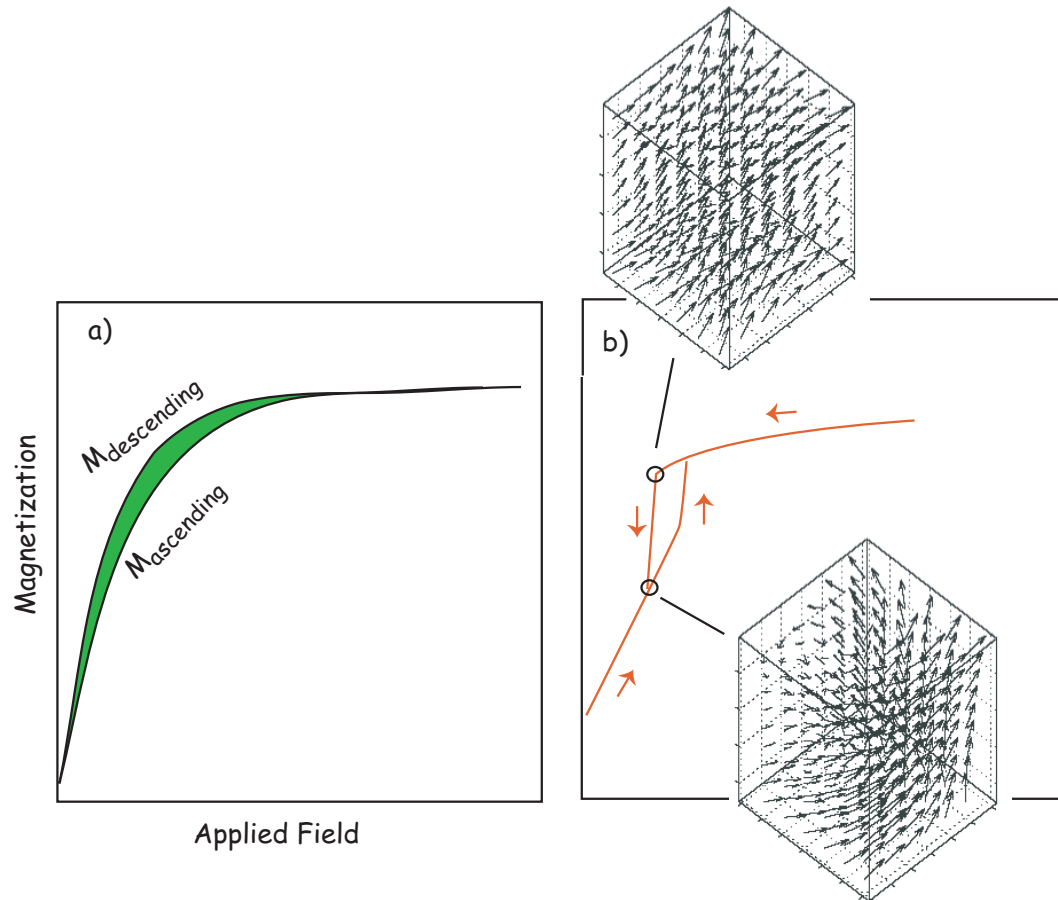


Figure 7.17: a) Illustration of a Zero FORC (ZFORC) whereby the descending loop from saturation is terminated at zero field and the field is then ramped back up to saturation. The transient hysteresis (TH) of Fabian (2003) is the shaded area between the two curves. b) Micromagnetic model of a ZFORC for a 100 nm cube of magnetite. Two snap shots of the internal magnetization on the descending and ascending loops are shown in the insets. [Figure redrawn from Yu and Tauxe, 2004.]

7.6 A glimpse at particle interaction

Much of the character of hysteresis loops is frequently attributed to interaction between particles, something that is extremely difficult to model and up until recently impossible to observe. A new technique for imaging of both the composition and the magnetization of particles on a nanoscale (e.g., Harrison et al. 2002) allows a glimpse at the magnetization structure of tiny, interacting particles. In Figure 7.18, we show an example of the mapping of iron and titanium (top panel) and the magnetic structure inferred from “off-axis electron holography” from Harrison et al. (2002). The figure shows both uniform magnetization and vortex structures within particles and super vortex structures from magnetostratic interaction fields between particles.

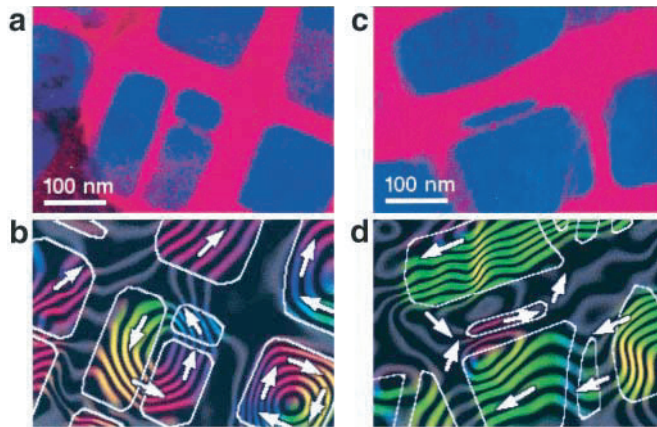


Figure 7.18: Top panel: chemical maps with iron in blue and titanium in red. These define the lamellar intergrowths of magnetite/ulvöspinel. Bottom panel: Associated magnetic microstructure. The arrows show the direction of magnetization inferred from off axis electron holography. [Figure from Harrison et al. 2002.]

A. SUPERPARAMAGNETISM

Appendix

A Superparamagnetism

The derivation of superparamagnetism follows closely that of paramagnetism whereby the probability of finding a magnetization vector an angle α away from the direction of the applied field is give by:

$$n(\alpha)d\alpha = 2\pi n_o e^{(\frac{M_s B v \cos \alpha}{kT})} \sin \alpha d\alpha. \quad (\text{A1})$$

The total magnetization contributed by the N moments is:

$$\frac{M}{M_s} = \int_0^\pi \cos \alpha n(\alpha) d\alpha. \quad (\text{A2})$$

Combining (A1) and (A2) we get

$$\begin{aligned} \frac{M}{M_s} &= N \frac{\int_0^\pi n(\alpha) \cos \alpha d\alpha}{\int_0^\pi n(\alpha) d\alpha} \\ &= N \frac{\int_0^\pi e^{(M_s B v \cos \alpha)/kT} \cos \alpha \sin \alpha d\alpha}{\int_0^\pi e^{(M_s B v \cos \alpha)/kT} \sin \alpha d\alpha}. \end{aligned}$$

By substituting $M_s B v / kT = \gamma$ and $\cos \alpha = x$, we write

$$\frac{M}{M_s} = N \frac{\int_1^{-1} e^{\gamma x} x dx}{\int_1^{-1} e^{\gamma x} dx} = N \left(\frac{e^\gamma + e^{-\gamma}}{e^\gamma - e^{-\gamma}} - \frac{1}{\gamma} \right) \quad (\text{A3})$$

and finally

$$\frac{M}{M_s} = N \left(\coth \gamma - \frac{1}{\gamma} \right). \quad (\text{A4})$$

where $\gamma = \frac{M_s B v}{kT}$ and N is the number of particles of volume v .